Intrinsic neural stem cell properties define brain hypersensitivity to genotoxic stress

Argyro Kalogeropoulou,[1] Maria Mougkogianni,[1,6] Marianna Iliadou,[1,6] Eleni Nikolopoulou,[1]
Stefanos Flordelis,[1] Alexandra Kanellou,[2] Marina Arbi,[2] Sofia Nikou,[3] Jadwiga Nieminuszczy,[4]
Wojciech Niedzwiedz,[4] Dimitrios Kardamakis,[5] Vasiliki Bravou,[3] Zoi Lygerou,[2] and Stavros Taraviras[1,*]

[1]Department of Physiology, School of Medicine, University of Patras, Basic Medical Sciences Building, 1 Askliepiou Str., University Campus, 26504, Rio, Patras, Greece
[2]Department of General Biology, School of Medicine, University of Patras, Patras, Greece
[3]Department of Anatomy-Histology-Embryology, School of Medicine, University of Patras, Patras, Greece
[4]The Institute of Cancer Research, London, UK
[5]Department of Radiation Oncology, School of Medicine, University of Patras, Patras, Greece
[6]These authors contributed equally
*Correspondence: taraviras@med.upatras.gr
https://doi.org/10.1016/j.stemcr.2022.04.018

SUMMARY

Impaired replication has been previously linked to growth retardation and microcephaly; however, why the brain is critically affected compared with other organs remains elusive. Here, we report the differential response between early neural progenitors (neuroepithelial cells [NECs]) and fate-committed neural progenitors (NPs) to replication licensing defects. Our results show that, while NPs can tolerate altered expression of licensing factors, NECs undergo excessive replication stress, identified by impaired replication, increased DNA damage, and defective cell-cycle progression, leading eventually to NEC attrition and microcephaly. NECs that possess a short G1 phase license and activate more origins than NPs, by acquiring higher levels of DNA-bound MCMs. *In vivo* G1 shortening in NPs induces DNA damage upon impaired licensing, suggesting that G1 length correlates with replication stress hypersensitivity. Our findings propose that NECs possess distinct cell-cycle characteristics to ensure fast proliferation, although these inherent features render them susceptible to genotoxic stress.

INTRODUCTION

Precise genome duplication is essential for the maintenance of genome integrity. DNA replication is tightly regulated by two consecutive processes, licensing and initiation of replication origins (Symeonidou et al., 2012). In mammalian cells, licensing is completed during the G1 phase with the recruitment of the MCM2–7 helicases (minichromosome maintenance) to the DNA resulting in thousands of competent origins of replication. During the S phase, replication initiates from a subset of the licensed origins, which are activated to establish a bidirectional replication fork. Over- or underlicensing causes slowing or stalling of the replication fork, which impedes DNA replication. This condition is described as replication stress and is associated with persistent DNA damage and chromosomal breaks fueling genomic instability (Petropoulos et al., 2019).

Maintaining genome stability is crucial for organismal growth and development and a prerequisite for tissue homeostasis in adult organisms. Replication stress-induced genomic instability has been widely associated with cancer (Gaillard et al., 2015), while recently, defective replication has also been implicated in developmental syndromes (Kalogeropoulou et al., 2019). Among the common symptoms of these syndromes is the smaller size of the head, a condi-

tion known as microcephaly, which is mainly attributed to incomplete formation of the cerebral cortex. Whereas microcephaly has been linked to a number of genetic factors implicated in cellular proliferation and maintenance of genomic stability (Jayaraman et al., 2018), the molecular mechanism underlying microcephaly upon impaired DNA replication remains elusive.

Cortical development begins very early in vertebrate embryogenesis, with the induction of the dorsal telencephalon from the most anterior region of the neural tube (Uzquiano et al., 2018). The dorsal telencephalon is populated by neuroepithelial cells (NECs), which perform rapid self-renewing divisions to establish the initial stem cell population of the developing cortex. With the onset of neurogenesis, NECs acquire a longer cell cycle and are gradually transformed into glial neural progenitors (NPs). NPs represent a fate-restricted population undergoing mainly asymmetric differentiative divisions to maintain their population but also to supply the cortical plate with neurons. An elongation of the G1 phase, which coincides with the establishment of NPs, plays a critical role in the switch to differentiation (Salomoni and Calegari, 2010).

To define the consequences of defective replication in cortical development, we investigated the response of early progenitors (herein referred to as NECs) and mid-neurogenesis progenitors (referred to as NPs) to impaired replication
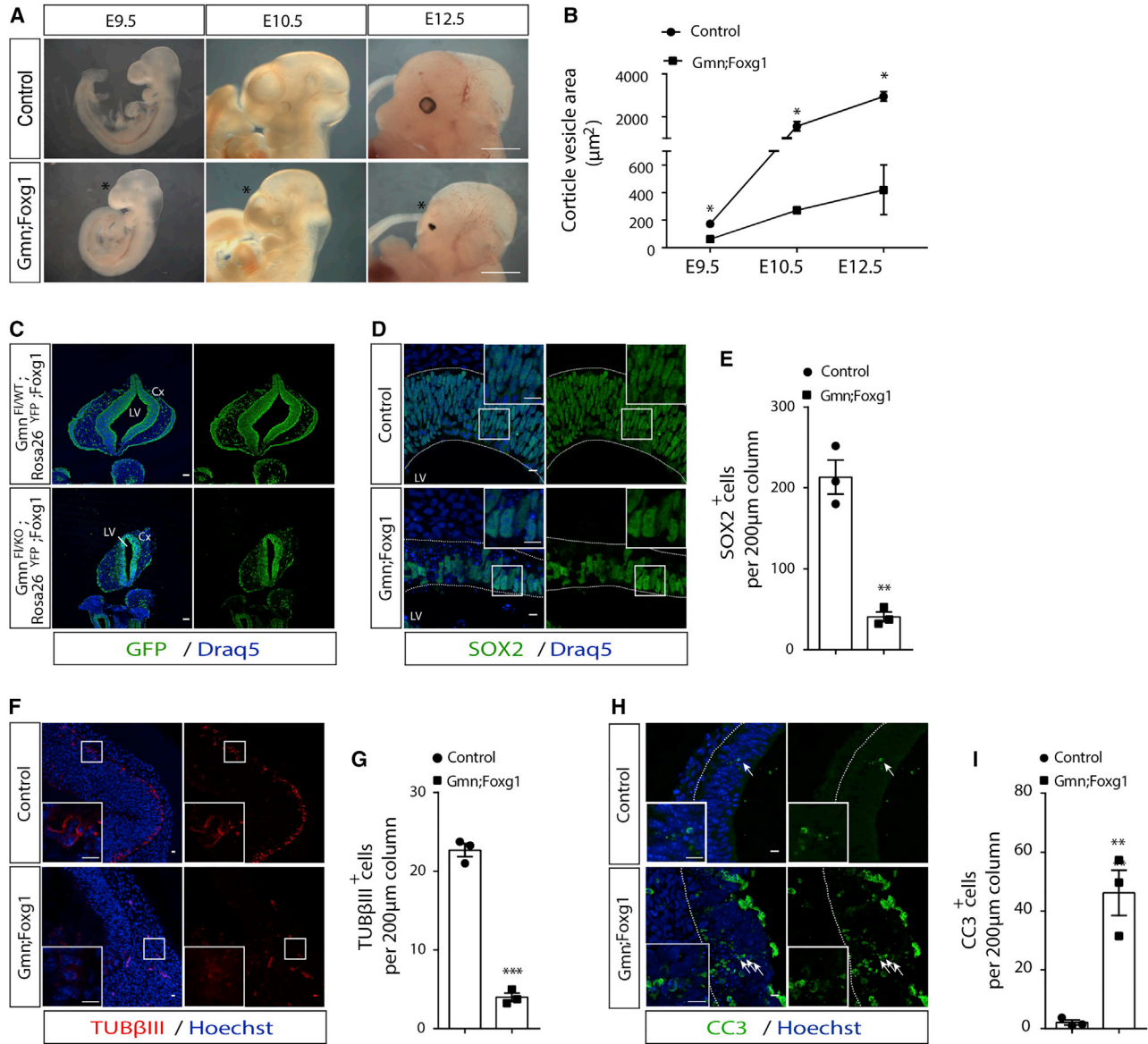
Figure 1. Impaired licensing of DNA replication in NECs results in severe microcephaly

(A) Lateral views of mouse embryos at different developmental stages. Note the marked decrease in the size of the telencephalic vesicles in Gmn;Foxg1 embryos (indicated by the black asterisks). Scale bars: 1 mm.

(B) The diagram depicts the mean ± SD telencephalic vesicle area of the indicated genotypes for the different developmental stages. Reduction in the telencephalic area of Gmn;Foxg1 embryos is statistically significant compared with control embryos (n = at least 4 mice/genotype and stage).

(C) Coronal brain sections of E9.5 embryos that carry a *Rosa26*[Fl-STOP-Fl-YFP] reporter cassette. The GFP fluorescence reports the efficient Foxg1-Cre-mediated recombination.

(D) Coronal brain sections of mouse embryos at E9.5 stained against Sox2 (green). The boxes indicate higher-magnification images of SOX2^{+} cells. Dotted lines delineate the cortical wall.

(E) The bar graph illustrates the number of SOX2^{+} cells in a 200-μm-wide column of the dorsal cortex. Mean ± SEM (n = 3/genotype).

(F) TUBβIII (red) in brain sections of E10.5 mouse embryos. Boxed areas indicate higher magnifications of representative cortical neurons.

(G) The graph shows the number of TUBβIII-expressing cells per 200-μm-wide column. Mean ± SEM (n = 3/genotype).

(legend continued on next page)

licensing by depleting Geminin (GMNN). GMNN is a known inhibitor of DNA replication licensing that is expressed in the proliferating neural stem and progenitor cells and is downregulated upon cell-cycle exit and differentiation (Spella et al., 2007). Previous studies have shown that suppression of GMNN in cultured cells induces aberrant licensing and incomplete genome replication (Huang et al., 2015; Klotz-Noack et al., 2012; Melixetian et al., 2004). Our results show that *in vivo* ablation of *Gmnn* from the rapidly proliferating NECs resulted in a severe microcephalic phenotype, while no similar effect was observed upon deletion from the fate-restricted NPs. In line with the phenotypic differences, NECs exhibited excessive replication stress, in contrast to NPs that remained unimpaired. To identify the underlying cause of the increased sensitivity of the rapidly proliferating cells to impaired licensing, we examined intrinsic differences between early- and mid-cortical progenitors. Collectively, our data suggest that the duration of the G1 and the distinct regulation of origin activity define two inherent features of the rapidly proliferating NECs that promote replicative stress upon impaired licensing, providing a mechanistic insight into the pathogenesis of replication-stress induced microcephaly.

RESULTS

In vivo licensing defects lead to reduced proliferation and apoptosis of NECs

To address the effect of impaired licensing during cortical development, we conditionally inactivated GMNN in the population of NECs. GMNN is a known regulator of DNA replication that acts by preventing the aberrant formation of the prereplicative complex and thus inhibits the unscheduled initiation of replication (Patmanidi et al., 2017).

To drive *Gmnn* depletion in NECs, mice homozygous for the floxed allele (*Gmnn^Fl/Fl*) were crossed with a mouse line carrying one functional and one null allele for *Gmnn* as well as the Foxg1-Cre transgene (*Gmnn^WT/KO;Foxg1-Cre*), which induces efficient recombination from the seven-somite stage (approximately embryonic day [E] 8.5–8.75). The conditional GMNN mutants *Gmnn^Fl/KO;Foxg1-Cre* (herein referred to as Gmn;Foxg1) exhibited a tremendous reduction in the size of the head and additional facial malformations, reminiscent of the microcephalic phenotype observed in humans (Figure 1A). Histopathological analysis revealed that the apparent reduction in head size was

due to incomplete expansion of the telencephalon (Figure S1A). Based on the surface area of the telencephalic vesicles, the cortex of the mutant embryos was decreased almost by 60% at E9.5 compared with control littermates. Further reduction at later developmental stages suggests the delayed development of the cortex (Figure 1B). Efficient Foxg1-Cre-mediated recombination at E9.5 was confirmed by GFP fluorescence in a mouse line carrying a *Rosa26^Fl-STOP-Fl-YFP* reporter (Figure 1C). Additional analysis by western blot established the efficient depletion of GMNN (Figure S1B). Importantly, the microcephalic phenotype was not observed in heterozygous embryos with or without Cre expression, which were used as controls (Figure S1C).

To determine the origins of microcephaly, we examined the expression of SOX2, one of the markers expressed by the initial stem cell population of the cortex. Sox2-expressing cells were significantly reduced in Gmn;Foxg1 embryos compared with control littermates (Figures 1D and 1E). An evident destruction in the organization of the SOX2+ cells was also observed in the cortex of the mutant embryos. Moreover, intraperitoneal (i.p.) administration of the thymidine analog CldU to the pregnant mice for 24 h revealed the reduced ability of the remaining SOX2+ NECs in the cortex of the Gmn;Foxg1 embryos to proliferate (Figures S1D and S1E). In line with the reduced generation of early NPs, formation of the early cortical neurons was also impaired. Cells expressing the neuronal marker β-tubulin III (TUBβIII) were identified in the basal surface of the cortex in the control embryos, whereas very few positive cells were detected in Gmn;Foxg1 embryos (Figures 1F and 1G).
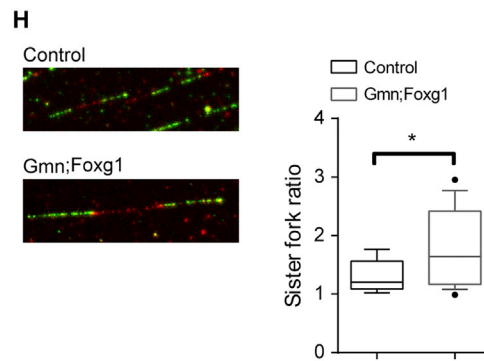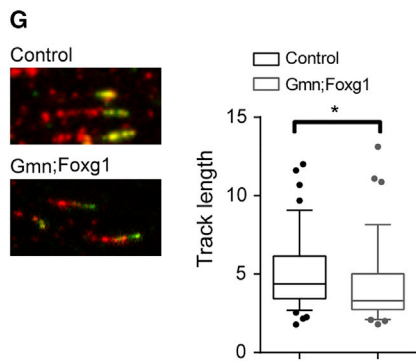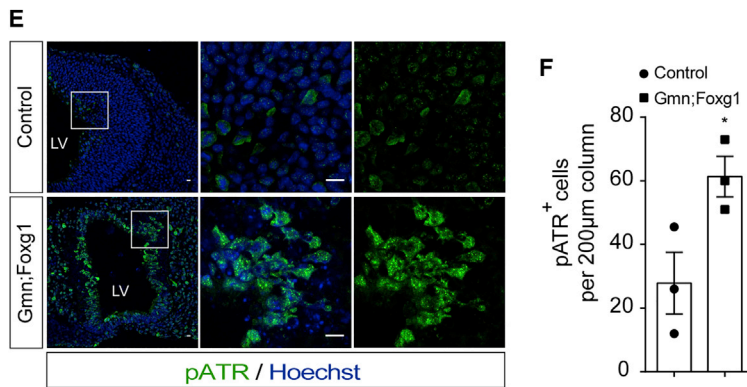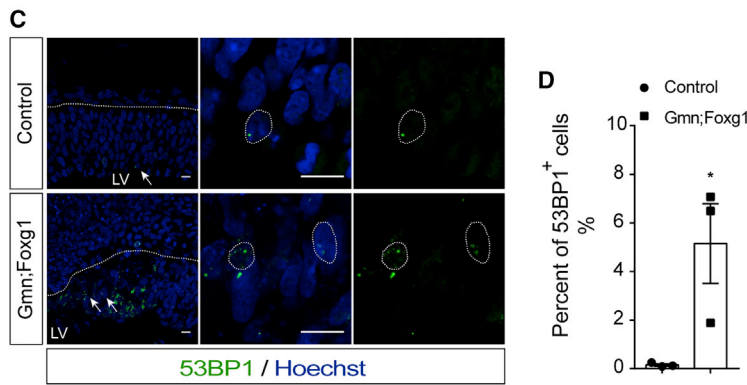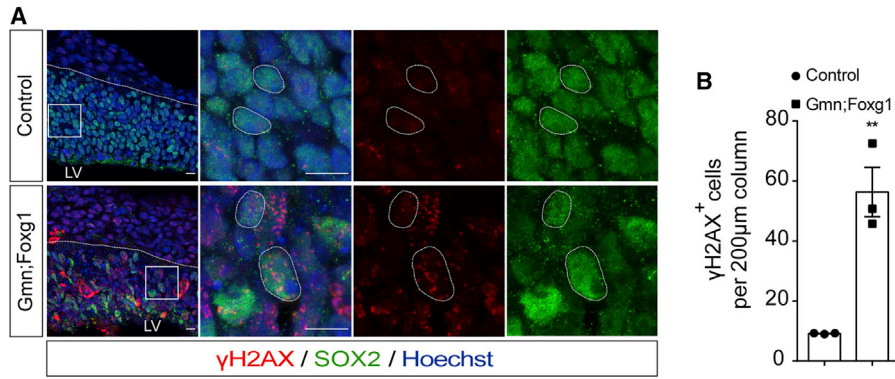
Because the microcephalic embryos exhibit deteriorated cortical morphology and reduced cell density, we examined for the presence of apoptosis. A marked increase in cells expressing the apoptotic marker cleaved caspase 3 (CC3) was identified in the cortex of Gmn;Foxg1 embryos (Figures 1H and 1I). Collectively, these data show that the initial pool of NECs is not efficiently formed in the GMNN-deficient embryos due to defective proliferation and apoptosis leading eventually to microcephaly.

Defective licensing in NECs leads to replication stress and cell-cycle aberrations

Persistent replication stress leads to the formation of excessive DNA damage and activation of the DNA damage response pathways (Técher et al., 2017). To identify

(H) Immunofluorescent staining for CC3 was performed in brain sections of E9.5 embryos. White arrows indicate apoptotic cells, which are presented in higher-magnification images.

(I) The bar graph depicts the number of CC3+ cells in a 200-μm-wide column. Mean ± SEM (n = 3/genotype). DNA was stained with Draq5 or Hoechst (blue). Scale bars: 50 μm for fluorescence images of whole-brain sections and 10 μm for higher-magnification images. *p ≤ 0.05, **p ≤ 0.01, ***p ≤ 0.001; t test. LV, lateral ventricle.

A

Control

Gmn;Foxg1

γH2AX / SOX2 / Hoechst

B

● Control
■ Gmn;Foxg1

γH2AX⁺ cells per 200μm column

C

Control

Gmn;Foxg1

53BP1 / Hoechst

D

● Control
■ Gmn;Foxg1

Percent of 53BP1⁺ cells %

E

Control

Gmn;Foxg1

pATR / Hoechst

F

● Control
■ Gmn;Foxg1

pATR⁺ cells per 200μm column

G

Control

Gmn;Foxg1

□ Control
□ Gmn;Foxg1

Track length

H

Control

Gmn;Foxg1

□ Control
□ Gmn;Foxg1

Sister fork ratio

(legend on next page)

whether GMNN depletion induces DNA damage in NECs, we initially examined the phosphorylation of histone H2AX (γH2AX) which marks the DNA at the site of damage. In parallel, Sox2 was used to ensure that only the proliferative NECs would be included in our analysis (Figure 2A). A significant increase in cells that displayed discernible γH2AX foci, which are indicative of double-strand breaks, was identified in the cortex of Gmn;Foxg1 embryos (Figure 2B). The formation of DNA lesions in the Gmn;Foxg1 embryos was also confirmed by the recruitment of the damage mediator protein 53BP1 in discrete foci (Schultz et al., 2000) (Figures 2C and 2D). Additional analysis showed that 53BP1[+] foci largely colocalize with γH2AX, indicating sites of DNA damage (Figure S2A). To further establish the induced DNA damage, we evaluated the expression of the phosphorylated form of ATR kinase (pATR), which is recruited in replication-induced lesions and orchestrates a coordinated cellular response (Saldivar et al., 2017) (Figure 2E). Interestingly, ATR phosphorylation was increased by almost 2-fold in Gmn;Foxg1 embryos, supporting a robust ATR activation (Figure 2F). Taken together, our data suggest that defective replication licensing in NECs drives excessive DNA damage and subsequent activation of DNA damage response mechanisms.

To study whether impaired replication is the main cause of the DNA damage observed in GMNN-depleted NECs, we performed DNA fiber analysis in cells derived from the embryos' cortexes. We observed shorter tracts in GMNN-depleted NECs compared with controls, suggesting fork slowing or stalling (Figure 2G). Moreover, the lengths of the sister CldU tracts in replication forks displayed significant asymmetry upon GMNN depletion, indicating fork stalling (Figure 2H). In line with these findings, we observed a mild increase in the initiation events when GMNN was absent, suggesting a generalized response to impaired licensing (Figure S2B). Taken together, these findings indicate that depletion of GMNN in NECs results in slowing and/or stalling of replication fork progression, which is prone to collapse, leading eventually to increased DNA lesions.

Excessive replication stress can lead to arrest of the cell cycle, providing the cell time to restore DNA damage and complete genome duplication before entering mitosis. To that end, we examined different phases of the cell cycle. A short (1 h) BrdU pulse was used for the identification of S-phase cells. Expression of the proliferative marker MKI67 was used in parallel to identify the cycling cells (Figure 3A). Gmn;Foxg1 embryos exhibited a significant reduction in the fraction of S-phase cells (BrdU[+]MKI67^{+}) compared with controls (Figure 3B). We next examined the mitotic entry of NECs. Based on the cell-cycle-dependent phosphorylation of histone 3 (pH3) (Hendzel et al., 1997), and the characteristic morphology of an interphase or a mitotic nucleus, we scored cells in G2 phase or in mitosis (Figure 3C). Gmn;Foxg1 embryos exhibited an increase in G2 cells, whereas mitotic cells were reduced by half compared with the control littermates (Figure 3D). These findings suggest that the NECs accumulate in G2 phase, being unable to successfully complete their cell cycle. Defects in cell-cycle progression were further assessed by a double pulse-chase experiment in which CldU and IdU were sequentially i.p. administered to the pregnant mice (Figures S2C–S2E).

To evaluate further the observed cell-cycle defects, we examined the mitotic progression of NECs. Whole telencephalic vesicles were dissected at E10.5 and subjected to whole-mount immunofluorescence using antibodies that recognize pericentrin, a centrosome marker, and β-catenin or α-tubulin to mark cell boundaries or spindle microtubules, respectively. In line with our previous findings, the mitotic cells that were identified in the apical surface of the cortex were reduced in the Gmn;Foxg1 embryos. Moreover, dividing cells with multipolar spindles were identified in Gmn;Foxg1 embryos, indicated by the

Figure 2. NECs undergo replication stress upon *in vivo* defective licensing

(A) Coronal brain sections of mouse embryos at E9.5 immunostained with anti-γH2AX (red) and anti-Sox2 (green). Cortical walls are restricted by the dotted lines. White boxes mark the higher-magnification images shown on the right. The demarcated cells represent positive cells. Note the γH2AX foci that are formed, representative of DNA damage.

(B) The graph depicts the γH2AX^{+} cells per 200-μm-wide area. Mean ± SEM (n = 3/genotype).

(C) Expression of 53BP1 (green) in the cortical wall of embryos at E10.5. The arrows indicate positive cells demarcated in higher-magnification images.
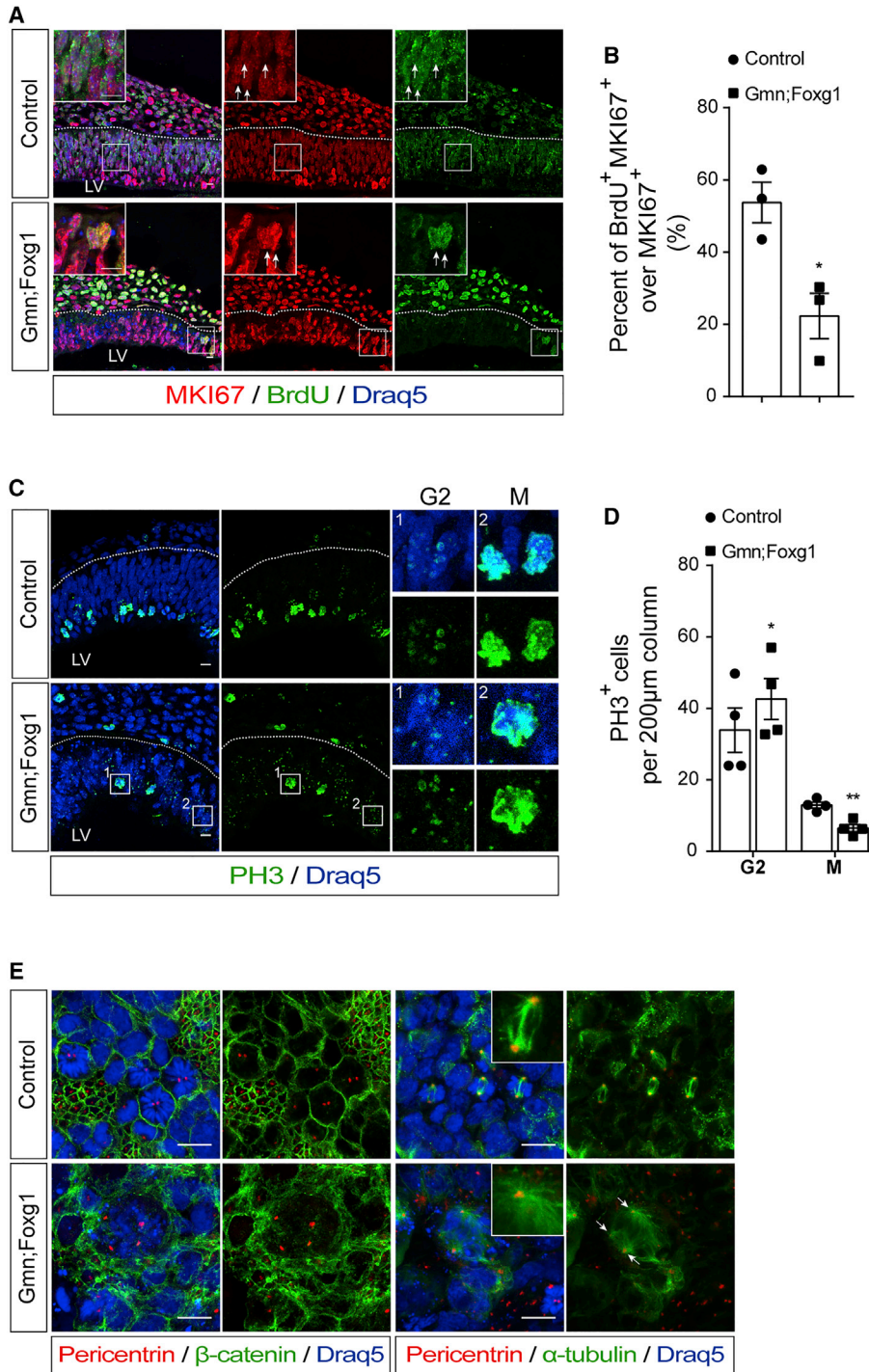
(D) The percentage of 53BP1-positive cells with >4 discernible foci per nucleus is presented in the bar graph. Mean ± SEM (n = 3/genotype).

(E) pATR (green) in brain sections of E9.5 embryos. The boxes indicate higher magnifications shown on the right.

(F) The graph shows the cells that express pATR per 200-μm-wide column. Mean ± SEM (n = 3/genotype).

(G) DNA fibers were spread from the cortexes of E10.5 embryos. The lengths of individual tracks were quantified and are presented in the graph (n = 46 control, n = 39 Gmn;Foxg1; data derived from two independent litters).

(H) The lengths of the green tracks in bidirectional forks were quantified in DNA fibers and the ratio of the sister forks is presented in the graph (n = 14 control, n = 19 Gmn;Foxg1; data derived from two independent litters). DNA is stained with Hoechst (blue). Scale bars: 10 μm. *p ≤ 0.05, **p ≤ 0.01; t test.

A

Control

Gmn;Foxg1

LV

MKI67 / BrdU / Draq5

B

● Control
■ Gmn;Foxg1

Percent of BrdU⁺ MKI67⁺ over MKI67⁺ (%)

C

Control

Gmn;Foxg1

LV

G2   M

PH3 / Draq5

D

● Control
■ Gmn;Foxg1

PH3⁺ cells per 200μm column

G2   M

E

Control

Gmn;Foxg1

Pericentrin / β-catenin / Draq5   Pericentrin / α-tubulin / Draq5

	Mitotic Index %	Multipolar divisions %
Control	13.82 ± 3.6 n=4841	-
Gmn;Foxg1	11.49 ± 3.2 n=2542	3.54

(legend on next page)

multiple centrosomes within cell nuclei (Figure 3E). Interestingly, multipolar divisions can occur as a consequence of mitotic delay, which has been associated with perturbed DNA replication (Hut et al., 2003). Together, our findings suggest that the GMNN-depleted NECs experience severe cell-cycle defects impeding their proliferation.

NPs are resilient to combined deregulation of licensing factors

NECs constitute the initial population of stem cells in the cortex until ∼E11.5, when they are gradually replaced by NPs that remain in the ventricular zone (VZ) until the end of the neurogenic phase (Mukhtar and Taylor, 2018). Previous studies by our group and others have shown that depletion of GMNN from NPs affects their cell-fate commitment but is not sufficient to cause gross brain aberrations (Schultz et al., 2011; Spella et al., 2011). To examine whether NPs experience basal levels of replication stress and DNA damage in the absence of GMNN, a previously established Nestin-Cre mouse line was used to drive GMNN depletion in NPs by E11.5 (Spella et al., 2011). In accordance with previous work, the *Geminin^{Fl/KO};NestinCre* (referred to as Gmn;Nestin) embryos are indistinguishable from control embryos, with no evident expression of γH2AX or CC3 in the cortexes of embryos at E14.5.

GMNN acts as an inhibitor of origin licensing by binding to the licensing factor CDT1 and thus preventing its association with chromatin during replication. Therefore, it is suggested that the relative levels of these two factors are critical for the maintenance of genomic integrity (Patmanidi et al., 2017). We hypothesized that CDT1 overexpression in GMNN-deficient NPs would compromise replication licensing and promote replication stress. To that end, we performed *in utero* electroporation to overexpress *CDT1-GFP* in NPs. CDT1 overexpression was confirmed in the transfected cells, identified as GFP+, by immunofluorescence (Figure 4C). We show that CDT1 overexpression could not affect the distribution of the transfected cells along the radial organization of the cortex, which is indicative of NP differentiation and migration toward the cortical plate (Figure 4D), and that the GFP+ cells were not expressing γH2AX in Gmn;Nestin or in control embryos, suggesting the absence of DNA lesions (Figure 4E).

Our findings show that depletion of GMNN alone or concomitant with CDT1 overexpression is not sufficient to induce DNA damage in NPs. In NECs, however, replication stress and DNA damage are identified very soon after GMNN depletion. Taken together, these data indicate that NECs and NPs respond differently to impaired licensing and demonstrate the sensitivity of rapidly proliferating cells to licensing defects compared with a more fate-restricted population.

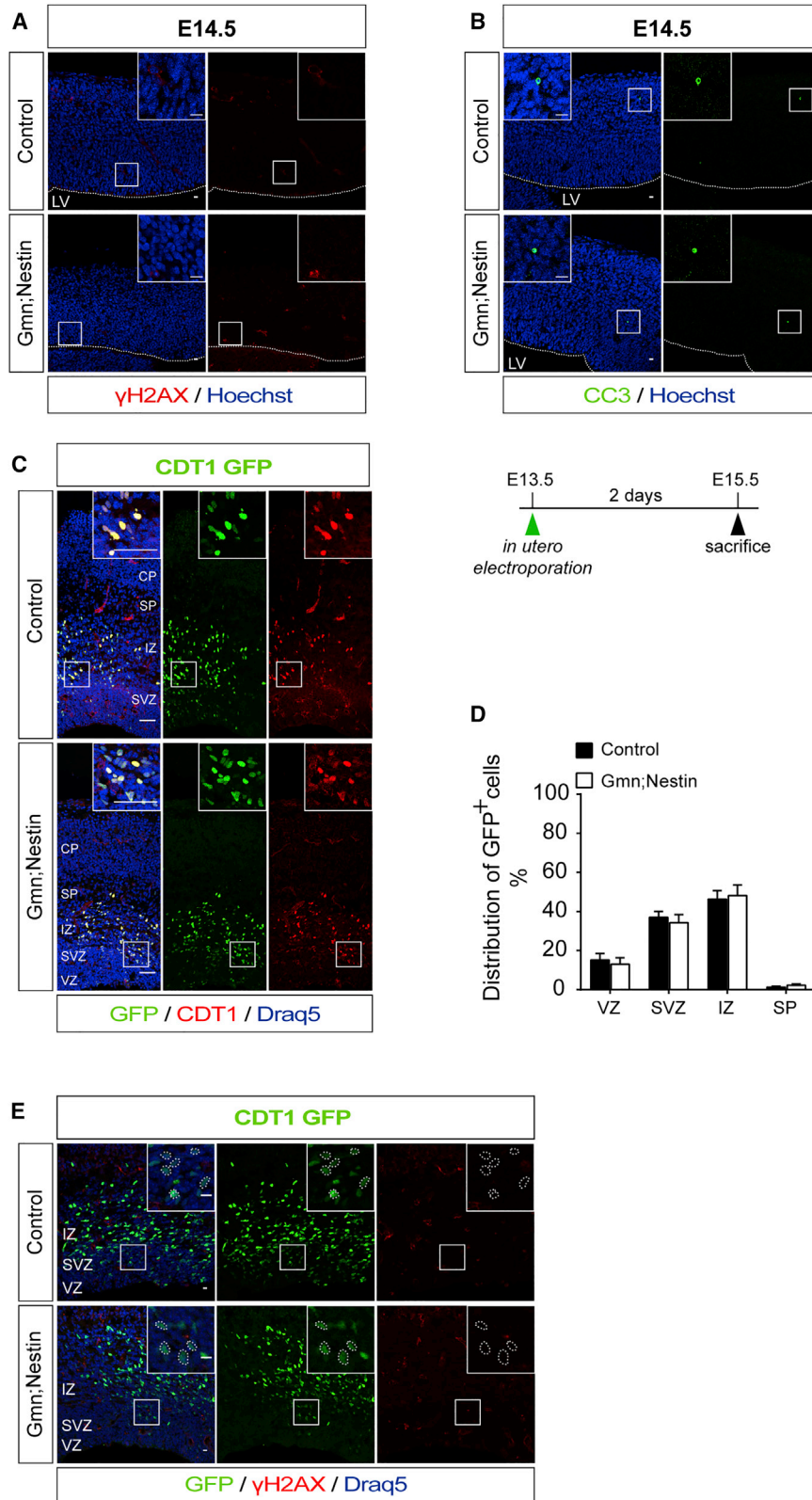## NECs utilize more origins than NPs during DNA replication

Eukaryotic cells can dynamically regulate initiation of DNA replication at spatial and temporal levels by the selective activation of replication origins (Fragkos et al., 2015). We, therefore, questioned whether cell-intrinsic differences in origin usage during DNA replication support the differential response between NECs and NPs to genotoxic stress. The density of activated origins was examined in DNA fibers prepared from freshly isolated cortexes of wild-type (WT) embryos at E10.5 or E14.5 to study the early population of NECs or NPs, respectively (Figure 5A). Importantly, the labeling of the nascent DNA strand was performed *in vivo* by i.p. injection of the two thymidine analogs to the mother, to avoid stress-induced artifacts during primary cell culture.

The interorigin distance (IOD), which decreases when more origins are activated, was 61.5 kb at E10.5, while it increased to 79.9 kb by E14.5, suggesting that NECs activate more origins compared with NPs (Figure 5C).

To further investigate origin usage, we examined the amount of chromatin-associated MCM2–7 complexes. Immunofluorescence against MCM2 was performed in non-ionic detergent-treated brain slices from embryos at E10.5 or E14.5, to allow the specific visualization of

Figure 3. Impaired cell proliferation due to cell-cycle defects is observed in NECs upon aberrant licensing
(A) BrdU (green) and MKI67 (red) staining in brain sections of embryos at E9.5. Dotted lines demarcate the cortical walls. Boxed areas are represented as higher-magnification images. White arrows point to double-positive cells.
(B) The graph presents the percentage of MKI67+ cells that incorporated BrdU. Mean ± SEM (n = 3/genotype).
(C) pH3 (green) staining in coronal brain sections derived from E9.5 embryos. Dotted lines delineate the cortical walls. Boxes indicate higher magnifications of positive cells. Note the spotted pattern of pH3 staining and the characteristic interphase nuclei representative of G2 cells (box 1) and the nuclear staining observed in condensed nuclei representative of mitotic cells (box 2).
(D) The bar graph depicts the number of pH3+ cells in a 200-μm-wide column assigned as G2 or M (mitotic) according to pH3 pattern. Mean ± SEM (n = 4/genotype).
(E) Whole telencephalic vesicles of embryo brains immunostained with antibodies for pericentrin (red) and β-catenin (green) or α-tubulin (green). Arrows point to the multiple centrosomes of one mitotic nucleus. The table shows the percentage of mitotic cells (mitotic index) and the percentage of mitoses with more than two centrosomes. n represents the number of cells analyzed per genotype. Data are derived from two independent litters. DNA is stained with Hoechst or Draq5 (blue). Scale bars: 10 μm. *p ≤ 0.05, **p ≤ 0.01; t test.

A E14.5

Control
Gmn;Nestin

LV
γH2AX / Hoechst

B E14.5

Control
Gmn;Nestin

LV
CC3 / Hoechst

C CDT1 GFP

Control
CP
SP
IZ
SVZ

Gmn;Nestin
CP
SP
IZ
SVZ
VZ

GFP / CDT1 / Draq5

E13.5 — 2 days — E15.5
in utero electroporation → sacrifice

D

Distribution of GFP$^+$ cells %

■ Control □ Gmn;Nestin

100
80
60
40
20
0
VZ SVZ IZ SP CP

E CDT1 GFP

Control
IZ
SVZ
VZ

Gmn;Nestin
IZ
SVZ
VZ

GFP / γH2AX / Draq5

(legend on next page)

chromatin-bound proteins, based on a novel experimental approach (Mougkogianni et al., 2021). A short EdU labeling was performed in parallel to distinguish different cell-cycle phases. In non-extracted tissues MCM2 marks all proliferating cells (Figure S3A) (Stoeber et al., 2001). Post extraction, however, MCM2 staining represents licensed origins in G1 cells (MCM2$^+$EdU$^-$) or cells undergoing S phase (MCM2$^+$EdU$^+$) (Figure 5D). Quantification of MCM2 fluorescence in G1 cells showed that NECs contain more chromatin-bound MCM2 than NPs (Figures 5E, S3B, and S3C). Together, our results suggest that NECs utilize more origins than NPs to complete DNA replication faithfully.

Forced G1 shortening elicits sensitivity to impaired licensing

Studies in *in vitro* systems have shown that the mechanism that mediates origin licensing is regulated according to the length of the G1 phase (Matson et al., 2017). Interestingly, NECs and NPs differ significantly in the duration of their G1, with the former exhibiting a shorter G1 relative to their cell cycle (Borrell and Calegari, 2014). Toward that direction, we questioned whether the increased sensitivity of NECs to genotoxic stress relates to their short G1 phase. To induce the selective modification of G1 phase in NPs *in vivo*, we overexpressed *CyclinE1-GFP* through *in utero* electroporation. It is known that CyclinE1 is rate limiting for the G1/S transition and it has been shown to force G1 shortening upon overexpression (Pilaz et al., 2009). Overexpression of CyclinE1 was confirmed in GFP$^+$ cells 2 days post electroporation (Figure S4A) and G1 shortening confirmed by the increase in GFP$^+$BrdU$^+$ cells, representing the transfected S-phase cells, at 14 h after electroporation with the CyclinE1-GFP plasmid (Figures 6A and 6B). To assess whether the shortening of the G1 is sufficient to induce replication stress in GMNN-depleted NPs, we examined DNA damage through immunofluorescence for γH2AX (Figure 6C). Our analysis showed a significant increase in the fraction of transfected cells that exhibited γH2AX foci in Gmn;Nestin embryos (Figure 6D), suggesting that a short G1 phase correlates with the sensitivity of neural precursors upon impaired licensing of DNA replication *in vivo*.

The link between G1 length and replication stress was also investigated in an inducible hTert-RPE1-CyclinE1 cell line (Figures S4B–S4F). Of note, DNA damage was further increased in CyclinE-overexpressing cells when GMNN was absent (Figures S4G and S4H). Overall, our findings support that cells with a short G1 are susceptible to defective DNA replication licensing and are in line with our observations from the two animal models.

DISCUSSION

Excessive replication stress is considered a source of genomic instability promoting malignant transformation. Inherited disorders caused by defective DNA replication present multiple developmental abnormalities in addition to increased cancer risk, suggesting that genomic instability is the underlying cause of the clinical features (Champeris Tsaniras et al., 2014; Petropoulos et al., 2019). Whereas the molecular basis of replication stress-induced genomic instability has been studied in the light of carcinogenesis (Champeris Tsaniras et al., 2018; Muñoz et al., 2017), this link remains poorly understood with respect to organismal development. Here, we provide evidence that defective licensing leads to replication stress and excessive DNA damage in NECs, causing destruction of brain development and microcephaly. Whereas our findings clearly support the idea that the replication stress induced by the depletion of GMNN is the primary cause of the microcephalic phenotype, a possible effect of GMNN absence and Foxg1 heterozygosity, induced by the specific Cre driver used in this study, cannot be completely excluded, and future studies are required to address this point.

We also show that the rapidly proliferating NECs display a marked sensitivity to impaired licensing compared with NPs, which represent a population of fate-restricted progenitors. Whereas NECs displayed replication defects and a marked increase in DNA damage upon GMNN depletion, leading to cell-cycle defects and eventually to apoptosis, neither deletion of GMNN nor concomitant deletion of GMNN and Cdt1 overexpression

Figure 4. DNA damage is not induced in NPs upon impaired licensing of replication
(A and B) Coronal brain sections of E14.5 embryos immunostained with anti-γH2AX (red) (A) and anti-caspase 3 (CC3, green) (B). Dotted lines demarcate the apical side of the cortical walls, and the white boxes indicate the higher magnifications shown in the insets.
(C) Embryos electroporated at E13.5 with a CDT1-GFP plasmid and isolated at E15.5. Brain sections were stained for GFP (green) and Cdt1 (red). The white boxes mark the higher-magnification images.
(D) The bar graph presents the percentage of transfected cells in each layer of the developing cortex over the total number of transfected cells. Mean ± SEM (n = 3/genotype). Not significant; t test.
(E) GFP (green) and γH2AX (red) in brain sections 2 days post electroporation. The insets present higher-magnification images, indicated by the white boxes. DNA is stained with Hoechst or Draq5 (blue). Scale bars: 10 μm. VZ, ventricular zone, SVZ, subventricular zone, IZ, intermediate zone.
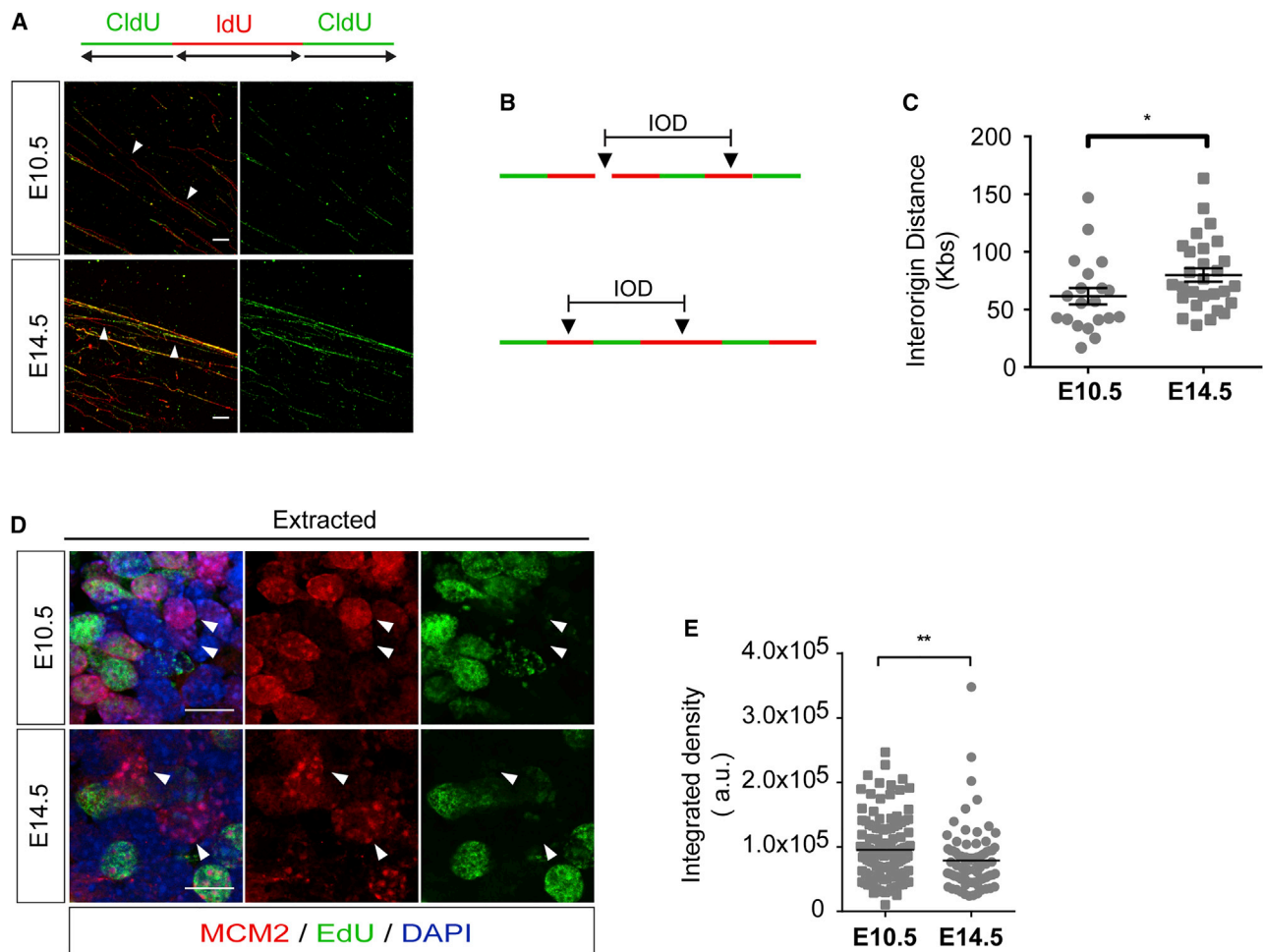
Figure 5. NECs utilize more origins than NPs to complete DNA replication

(A) The scheme shows the sequential incorporation of IdU (red) and CldU (green) in a fired origin. Representative images of DNA fiber spreads derived from WT embryos at E10.5 and E14.5 are shown. White arrowheads indicate structures of DNA replication origins activated during the first pulse.

(B and C) Schematic representation of DNA fiber structures showing two adjacent DNA replication origins. The distance between two adjacent origins is marked as the interorigin distance (IOD) (B). Interorigin distances in DNA fibers were quantified and are depicted in the graph (C). Data were obtained from two independent experiments (~30 pairs of consecutive origins/condition; five embryos per condition in each experiment). Mean ± SEM. *p ≤ 0.05; Mann-Whitney.

(D) Vibratome sections of embryo brains at E10.5 and E14.5 were subjected to a pre-extraction protocol and immunofluorescent staining with antibodies against MCM2 (red) and EdU (green). White arrowheads point to cells in G1 identified as MCM2$^+$EdU$^-$. DNA was stained with DAPI (blue).

(E) The graph shows the intensity of MCM2 per cell in vibratome sections. The line represents the mean value for each group. Data from one representative experiment are presented in the graph (~100 cells/condition). **p ≤ 0.01; Mann-Whitney. Two more independent experiments were performed and the data are presented in Figure S3C. Scale bars: 10 μm.

in NPs were sufficient to induce DNA damage. The absence of replication stress in NPs upon the combined deregulation of both factors, which is known to induce re-replication in a variety of cellular systems (Li and Blow, 2005; Nishitani et al., 2001; Stathopoulou et al., 2012), demonstrates that NPs can efficiently respond to impaired licensing. Our data propose that the accumula-

tion of CDT1 upon GMNN absence is not the sole cause of the differential response between NECs and NPs, as this would cause at least a moderate effect in GMNN-depleted NPs after CDT1 overexpression. However, we cannot rule out the possibility that NPs rely on alternative pathways for Cdt1 regulation (Li et al., 2003; Nishitani et al., 2006).
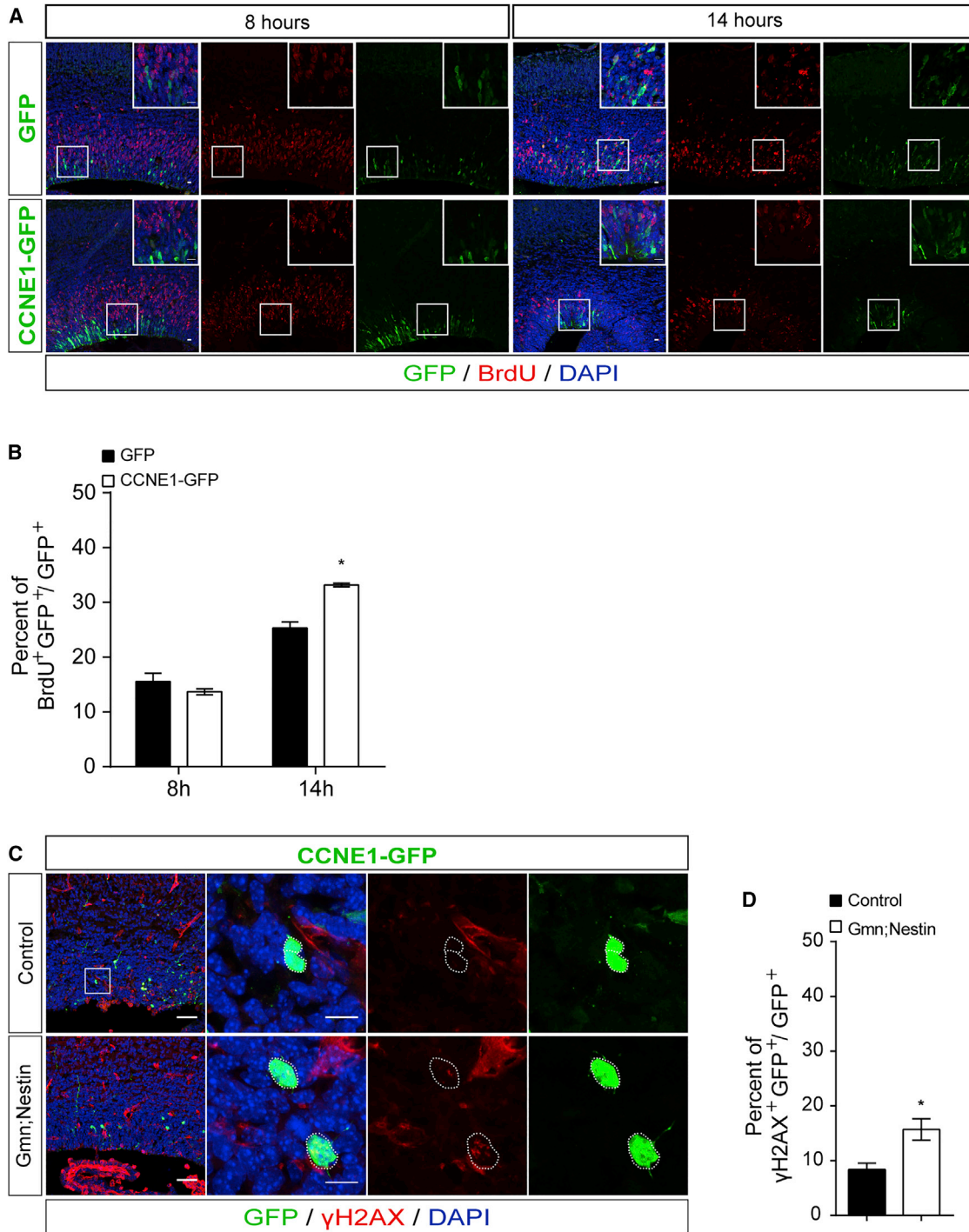
Figure 6. A short G1 phase elicits increased DNA damage upon aberrant initiation of DNA replication

(A) A CyclinE1-GFP (CCNE1-GFP) construct or an empty GFP vector was introduced through *in utero* electroporation into the lateral ventricle of embryos at E14.5. BrdU was i.p. injected into females for 1 h before sacrifice. White boxes indicate the higher-magnification images. GFP (green) and BrdU (red) staining in brain sections at 8 or 14 h post electroporation is shown. Scale bars: 10 μm.

(B) The percentage of BrdU$^+$GFP$^+$ cells over the total number of transfected cells is presented in the bar graph. Mean ± SEM (n = 3/embryos per condition).

(legend continued on next page)

Previous studies have established that DNA replication is dynamically regulated among different cell types and developmental stages to ensure the complete error-free duplication of the genome (Buckley et al., 2015; Hiratani et al., 2008). Here, we show that NECs possess more MCM2–7 complexes on their chromatin and activate more origins to complete DNA replication compared with NPs. In accordance with our findings, undifferentiated embryonic stem cells (ESCs) license and activate more origins than fate-restricted NPs (Ge et al., 2015; Rausch et al., 2020), suggesting that the increased usage of origins is an inherent feature of multipotent stem cells that is abrogated upon fate commitment.

Our work suggests that the activation of more origins in NECs could, possibly, contribute to the susceptibility of these cells to licensing defects. Mammalian cells preserve a reservoir of licensed origins, namely dormant, which are activated upon perturbed replication to cover unreplicated segments (Ge et al., 2007; Ibarra et al., 2008). We hypothesize that the increased activation of origins in NECs consequently results in limited backup origins as well as restricted replication building blocks (Poli et al., 2012; Toledo et al., 2013) and thus, the completion of DNA replication is prevented under perturbed conditions, leading to excessive replicative stress. Accordingly, NPs, which physiologically use fewer origins, possess a sufficient backup of origins to complete genome duplication upon replication impairment. In line with our hypothesis, it has been shown that limiting origin licensing *in vitro* causes aberrant DNA replication and DNA damage in NSCs (neural stem cells) (Ge et al., 2015). Of note, similar effects have also been observed in the hematopoietic system, where the decrease in licensed origins promotes replication stress in hematopoietic stem cells and not in committed progenitor populations, suggesting that excess origin licensing is also essential for other tissue-specific stem cells (Alvarez et al., 2015; Pruitt et al., 2007).

Accumulating evidence proposes that origin licensing, G1 duration, and multipotency are interlinked cellular features (Coronado et al., 2013; Matson et al., 2017). We have shown here that NECs and NPs differ in the number of origins that activate during DNA replication. Moreover, early and mid-NPs exhibit significant differences in the duration of their G1, which lasts ∼9 h in early progenitors and ∼12 h in mid-progenitors (Calegari et al., 2005; Takahashi et al., 1995). By inducing G1 shortening *in vivo*, we show here that a short G1 phase is a feature that can compromise genome integrity upon exposure to genotoxic stress. In fact, it has been proposed that some oncogenes promote genomic instability by forcing the shortening of G1 phase (Costantino et al., 2014; Macheret and Halazonetis, 2018).

Whereas GMNN plays a critical role in the regulation of DNA replication licensing, it is also implicated in cell-fate commitment by modulating the chromatin state and the transcriptional activation of lineage-specific genes (Del Bene et al., 2004; Karamitros et al., 2015; Kroll et al., 1998; Luo et al., 2004; Patterson et al., 2014; Seo et al., 2005; Yellajoshyula et al., 2011). Interestingly, previous *in vivo* studies in the hematopoietic system (Karamitros et al., 2010, 2015) and in the adult brain (Sankar et al., 2017; Schultz et al., 2011) support the idea that GMNN functions depend on the cellular context. Here, by using two distinct transgenic animal models, we describe the differential response of NECs and neurogenic NPs to GMNN depletion. In line with our previous work by Spella et al. (2011), our findings point out that GMNN exerts diverse roles across brain development, as it is indispensable for the regulation of DNA replication licensing in NECs, while it regulates proliferation and differentiation decisions in NPs.

NSC elimination due to proliferation defects or cell death is a common feature of several microcephalic mouse models (Marjanović et al., 2015; Marthiens et al., 2013). Our data here propose that impaired licensing and the subsequent replication stress-induced DNA damage in GMNN-deficient NECs is the primary cause of the observed microcephaly. Intriguingly, mutations in GMNN and other licensing factors have been linked to microcephaly or other brain malformations in humans, pointing out the importance of faithful genome duplication during cortical development (Burrage et al., 2015; de Munnik et al., 2012; Ravindran et al., 2021; Vetro et al., 2017).

In conclusion, our analysis supports the differential susceptibility between NECs and NPs to licensing defects, pointing out the vulnerability of rapidly proliferating stem cells to intrinsically induced genotoxic stress. In line with our findings, previous studies have shown that adult neural stem cells are more prone to malignant transformation induced by tumor suppressor loss compared with more differentiated cells (Alcantara Llaguno et al., 2019). Elucidating the distinct regulation of licensing in rapidly proliferating cells and the consequences of impaired licensing in these populations will undeniably pave the way toward our understanding of genomic instability diseases and will provide new grounds of research in the design of cancer stem cell-targeting therapies.

(C) GFP (green) and γH2AX (red) in brain sections at 2 days post electroporation. White boxes indicate the higher-magnification images. Scale bars: 50 μm in lower-magnification and 10 μm in higher-magnification images.

(D) The bar graph presents the percentage of γH2AX$^+$GFP$^+$ over the total number of GFP$^+$ cells. Mean ± SEM (n = 3/genotype). DNA was stained with DAPI. *p ≤ 0.05; t test.

EXPERIMENTAL PROCEDURES

Mouse knockout strains

Geminin$^{flox/flox}$, *Geminin*$^{flox/flox}$;*Rosa26*$^{fl-STOP-fl-YFP}$, *Geminin*$^{WT/KO}$; *Foxg1-Cre*, and *Geminin*$^{WT/KO}$;*NestinCre* inbred mouse lines and WT mice used for this study were housed in the animal house of the University of Patras (EL-13-BIOexp04). All animal-related procedures were conducted in strict accordance with EU directives and approved by the Veterinary Administrations of the Prefecture of Achaia, Greece, and by the Research Ethics Committee of the University of Patas, Greece. For details in mice husbandry and genotyping see the supplemental experimental procedures.

Incorporation and detection of thymidine analogs

For *in vivo* labeling of the S phase the mice were injected with 100 μg of BrdU (B9285, Sigma) per gram of the animal's weight or with 100 μg of EdU (A10044, Invitrogen) and sacrificed 1 h later. For double labeling, 100 μg of CldU (C6891, Sigma) and of IdU (I7125, Sigma) per gram of the animal's weight was injected i.p. into the mice, separated by 23 h from each other. For the detection of BrdU, CldU, and IdU the samples were treated with 2 N HCl for 30 min at 37°C and subsequently processed for immunofluorescent staining. EdU was detected by click chemistry according to the manufacturer's instructions (Baseclick), followed by immunofluorescence.

In utero electroporation

In utero electroporation was performed at E14.5 as previously described. Mice were sacrificed 48 h after surgery to collect the embryos. More details of the protocol and a list with the constructs used in this work are provided in the supplemental experimental procedures.

Immunohistochemistry

Whole embryos or embryonic brains were dissected at the appropriate gestation day depending on the experimental procedure. Embryos were defined as E0.5 on the morning of the day of the vaginal plug. Details on tissue preparation and staining protocols are provided the supplemental experimental procedures.

Dissection and immunofluorescence of cortical explants

Telencephalic vesicles were dissected from E10.5 embryos in room temperature 1× PBS as described previously (Rujano et al., 2015). Dissected vesicles were treated with 0.1% Triton X-100 for 3 min followed by fixation with 4% paraformaldehyde (PFA) for 1 h at room temperature. Subsequently, the tissues were incubated in 1% Triton X-100 for 5 min and blocked in 3% BSA, 1% normal goat serum, and 0.3% Triton X-100 in PBS for 1 h. Incubation with the primary or secondary antibodies (dilution 1:1,000) was performed overnight at 4°C. DNA was stained with Draq5 (Biostatus). Following staining, the dorsal part of the telencephalic vesicles was carefully isolated, exposing the apical surface, and mounted on a glass coverslip using Mowiol 4-88 (Calbiochem).

Pre-extraction and immunofluorescence of brain slices

Preparation of acute brain slices was performed as previously described (Mougkogianni et al., 2021). Images were acquired in a confocal microscope with a step size 0.7 μm and a total z volume of 7.608 μm^3. Fluorescence intensity was measured with the ImageJ software and depicted in arbitrary units. The rolling ball algorithm was used to subtract the background before quantification.

DNA fiber assay

For DNA fiber analysis, pregnant mice were subjected to i.p. injection of 20 mM IdU (10 μL/g body weight) followed by an i.p. injection of 100 mM CldU (10 μL/g body weight) after 20 min. The mice were sacrificed after 10 min and the embryos were isolated and placed in ice-cold PBS. The dorsal cortex from E10.5 embryos or the ventricular/subventricular zones from E14.5 embryos were isolated, and single-cell suspensions were prepared (7×10^2 cells/μL for E10.5 embryos and 22×10^2 cells/μL for E14.5 embryos). For the DNA fibers from the conditional knockout embryos and the respective controls, cortexes were dissected and cultured with each thymidine analog sequentially. DNA fiber spreads were prepared and stained as previously described (Nieminuszczy et al., 2016). Details on the microscopy analysis performed on DNA fibers are provided in the supplemental experimental procedures.

Data analysis

The significance of the difference between the examined populations was determined by unpaired two-tailed t test or Mann-Whitney test. Differences were regarded as significant by p value. All statistical analyses and graph preparation were performed in GraphPad Prism 6. Additional information on microscopy analyses performed in this work is provided in the supplemental experimental procedures.

AUTHOR CONTRIBUTIONS

A.K. designed the study, performed experiments, performed data analysis and interpretation, and wrote the paper. M.M., M.I., E.N., S.F., and S.N. performed experiments. A.K., A.M., and J.N. contributed to the establishment of protocols and performed experiments. W.N., D.K., and V.B. interpreted and discussed the results. Z.L. designed the study and interpreted and discussed the results. S.T. designed the study, performed data analysis and interpretation, and wrote the paper.

CONFLICTS OF INTERESTS

The authors declare no competing interests.

ACKNOWLEDGMENTS

REFERENCES

Alcantara Llaguno, S., Sun, D., Pedraza, A.M., Vera, E., Wang, Z., Burns, D.K., and Parada, L.F. (2019). Cell-of-origin susceptibility to glioblastoma formation declines with neural lineage restriction. Nat. Neurosci. *22*, 545–555. https://doi.org/10.1038/s41593-018-0333-8.

Alvarez, S., Díaz, M., Flach, J., Rodriguez-Acebes, S., López-Contreras, A.J., Martínez, D., Cañamero, M., Fernández-Capetillo, O., Isern, J., Passegué, E., and Mendez, J. (2015). Replication stress caused by low MCM expression limits fetal erythropoiesis and hematopoietic stem cell functionality. Nat. Commun. *6*, 8548. https://doi.org/10.1038/ncomms9548.

Borrell, V., and Calegari, F. (2014). Mechanisms of brain evolution: regulation of neural progenitor cell diversity and cell cycle length. Neurosci. Res. *86*, 14–24. https://doi.org/10.1016/j.neures.2014.04.004.

Rivera-Mulia, J.C., Sasaki, T., Zimmerman, J., Didier, R.A., Nazor, K., Loring, J.F., Lian, Z., Weissman, S., Robins, A.J., Schulz, T.C., Menendez, L., Kulik, M.J., Dalton, S., Gabr, H., Kahveci, T., and Gilbert, D.M. (2015). Dynamic changes in replication timing and gene expression during lineage specification of human pluripotent stem cells. Genome Res. *25*, 1091–1103. https://doi.org/10.1101/gr.187989.114.

Burrage, L.C., Charng, W.-L., Eldomery, M.K., Willer, J.R., Davis, E.E., Lugtenberg, D., Zhu, W., Leduc, M.S., Akdemir, Z.C., Azamian, M., et al. (2015). De novo GMNN mutations cause autosomal-dominant primordial dwarfism associated with Meier-Gorlin syndrome. Am. J. Hum. Genet. *97*, 904–913. https://doi.org/10.1016/j.ajhg.2015.11.006.

Calegari, F., Haubensak, W., Haffner, C., and Huttner, W.B. (2005). Selective lengthening of the cell cycle in the neurogenic subpopulation of neural progenitor cells during mouse brain development. J. Neurosci. Off. J. Soc. Neurosci. *25*, 6533–6538. https://doi.org/10.1523/JNEUROSCI.0778-05.2005.

Champeris Tsaniras, S., Kanellakis, N., Symeonidou, I.E., Nikolopoulou, P., Lygerou, Z., and Taraviras, S. (2014). Licensing of DNA replication, cancer, pluripotency and differentiation: an interlinked world? Semin. Cell Dev. Biol. *30*, 174–180. https://doi.org/10.1016/j.semcdb.2014.03.013.

Champeris Tsaniras, S., Villiou, M., Giannou, A.D., Nikou, S., Petropoulos, M., Pateras, I.S., Tserou, P., Karousi, F., Lalioti, M.-E., Gorgoulis, V.G., et al. (2018). Geminin ablation *in vivo* enhances tumorigenesis through increased genomic instability. J. Pathol. *246*, 134–140. https://doi.org/10.1002/path.5128.

Coronado, D., Godet, M., Bourillot, P.-Y., Tapponnier, Y., Bernat, A., Petit, M., Afanassieff, M., Markossian, S., Malashicheva, A., Iacone, R., et al. (2013). A short G1 phase is an intrinsic determinant of naïve embryonic stem cell pluripotency. Stem Cell Res. *10*, 118–131. https://doi.org/10.1016/j.scr.2012.10.004.

Costantino, L., Sotiriou, S.K., Rantala, J.K., Magin, S., Mladenov, E., Helleday, T., Haber, J.E., Iliakis, G., Kallioniemi, O.P., and Halazonetis, T.D. (2014). Break-induced replication repair of damaged forks induces genomic duplications in human cells. Science *343*, 88–91. https://doi.org/10.1126/science.1243211.

de Munnik, S.A., Bicknell, L.S., Aftimos, S., Al-Aama, J.Y., van Bever, Y., Bober, M.B., Clayton-Smith, J., Edrees, A.Y., Feingold, M., Fryer, A., et al. (2012). Meier-Gorlin syndrome genotype-phenotype studies: 35 individuals with pre-replication complex gene mutations and 10 without molecular diagnosis. Eur. J. Hum. Genet. EJHG *20*, 598–606. https://doi.org/10.1038/ejhg.2011.269.

Bene, F.D., Tessmar-Raible, K., and Wittbrodt, J. (2004). Direct interaction of geminin and Six3 in eye development. Nature *427*, 745–749. https://doi.org/10.1038/nature02292.

Fragkos, M., Ganier, O., Coulombe, P., and Méchali, M. (2015). DNA replication origin activation in space and time. Nat. Rev. Mol. Cell Biol. *16*, 360–374. https://doi.org/10.1038/nrm4002.

Gaillard, H., García-Muse, T., and Aguilera, A. (2015). Replication stress and cancer. Nat. Rev. Cancer *15*, 276–289. https://doi.org/10.1038/nrc3916.

Ge, X.Q., Han, J., Cheng, E.-C., Yamaguchi, S., Shima, N., Thomas, J.-L., and Lin, H. (2015). Embryonic stem cells license a high level of dormant origins to protect the genome against replication stress. Stem Cell Rep. *5*, 185–194. https://doi.org/10.1016/j.stemcr.2015.06.002.

Ge, X.Q., Jackson, D.A., and Blow, J.J. (2007). Dormant origins licensed by excess Mcm2–7 are required for human cells to survive replicative stress. Genes Dev. *21*, 3331–3341. https://doi.org/10.1101/gad.457807.

Hendzel, M.J., Wei, Y., Mancini, M.A., Van Hooser, A., Ranalli, T., Brinkley, B.R., Bazett-Jones, D.P., and Allis, C.D. (1997). Mitosis-specific phosphorylation of histone H3 initiates primarily within pericentromeric heterochromatin during G2 and spreads in an ordered fashion coincident with mitotic chromosome condensation. Chromosoma *106*, 348–360. https://doi.org/10.1007/s004120050256.

Hiratani, I., Ryba, T., Itoh, M., Yokochi, T., Schwaiger, M., Chang, C.-W., Lyou, Y., Townes, T.M., Schübeler, D., and Gilbert, D.M. (2008). Global reorganization of replication domains during

embryonic stem cell differentiation. PLoS Biol. *6*, e245. https://doi.org/10.1371/journal.pbio.0060245.

Huang, Y.-Y., Kaneko, K.J., Pan, H., and DePamphilis, M.L. (2015). Geminin is essential to prevent DNA Re-Replication-Dependent apoptosis in pluripotent cells, but not in differentiated cells. Stem Cells *33*, 3239–3253. https://doi.org/10.1002/stem.2092.

Hut, H.M.J., Lemstra, W., Blaauw, E.H., van Cappellen, G.W.A., Kampinga, H.H., and Sibon, O.C.M. (2003). Centrosomes split in the presence of impaired DNA integrity during mitosis. Mol. Biol. Cell *14*, 1993–2004. https://doi.org/10.1091/mbc.E02-08-0510.

Ibarra, A., Schwob, E., and Méndez, J. (2008). Excess MCM proteins protect human cells from replicative stress by licensing backup origins of replication. Proc. Natl. Acad. Sci. U S A *105*, 8956–8961. https://doi.org/10.1073/pnas.0803978105.

Jayaraman, D., Bae, B.-I., and Walsh, C.A. (2018). The genetics of primary microcephaly. Annu. Rev. Genom. Hum. Genet. *19*, 177–200. https://doi.org/10.1146/annurev-genom-083117-021441.

Kalogeropoulou, A., Lygerou, Z., and Taraviras, S. (2019). Cortical development and brain malformations: insights from the differential regulation of early events of DNA replication. Front. Cell Dev. Biol. *7*, 29. https://doi.org/10.3389/fcell.2019.00029.

Karamitros, D., Kotantaki, P., Lygerou, Z., Veiga-Fernandes, H., Pachnis, V., Kioussis, D., and Taraviras, S. (2010). Differential geminin requirement for proliferation of thymocytes and mature T cells. J. Immunol. *184*, 2432–2441. Baltim. Md 1950. https://doi.org/10.4049/jimmunol.0901983.

Karamitros, D., Patmanidi, A.L., Kotantaki, P., Potocnik, A.J., Bähr-Ivacevic, T., Benes, V., Lygerou, Z., Kioussis, D., and Taraviras, S. (2015). Geminin deletion increases the number of fetal hematopoietic stem cells by affecting the expression of key transcription factors. Dev. Camb. Engl. *142*, 70–81. https://doi.org/10.1242/dev.109454.

Klotz-Noack, K., McIntosh, D., Schurch, N., Pratt, N., and Blow, J.J. (2012). Re-replication induced by geminin depletion occurs from G2 and is enhanced by checkpoint activation. J. Cell Sci. *125*, 2436–2445. https://doi.org/10.1242/jcs.100883.

Kroll, K.L., Salic, A.N., Evans, L.M., and Kirschner, M.W. (1998). Geminin, a neuralizing molecule that demarcates the future neural plate at the onset of gastrulation. Dev. Camb. Engl. *125*, 3247–3258. https://doi.org/10.1242/dev.125.16.3247.

Li, A., and Blow, J.J. (2005). Cdt1 downregulation by proteolysis and geminin inhibition prevents DNA re-replication in Xenopus. EMBO J. *24*, 395–404. https://doi.org/10.1038/sj.emboj.7600520.

Li, X., Zhao, Q., Liao, R., Sun, P., and Wu, X. (2003). The SCF(Skp2) ubiquitin ligase complex interacts with the human replication licensing factor Cdt1 and regulates Cdt1 degradation. J. Biol. Chem. *278*, 30854–30858. https://doi.org/10.1074/jbc.C300251200.

Luo, L., Yang, X., Takihara, Y., Knoetgen, H., and Kessel, M. (2004). The cell-cycle regulator geminin inhibits Hox function through direct and polycomb-mediated interactions. Nature *427*, 749–753. https://doi.org/10.1038/nature02305.

Macheret, M., and Halazonetis, T.D. (2018). Intragenic origins due to short G1 phases underlie oncogene-induced DNA replication stress. Nature *555*, 112–116. https://doi.org/10.1038/nature25507.

Marjanović, M., Sánchez-Huertas, C., Terré, B., Gómez, R., Scheel, J.F., Pacheco, S., Knobel, P.A., Martínez-Marchal, A., Aivio, S., Palenzuela, L., et al. (2015). CEP63 deficiency promotes p53-dependent microcephaly and reveals a role for the centrosome in meiotic recombination. Nat. Commun. *6*, 7676–7714. https://doi.org/10.1038/ncomms8676.

Marthiens, V., Rujano, M.A., Pennetier, C., Tessier, S., Paul-Gilloteaux, P., and Basto, R. (2013). Centrosome amplification causes microcephaly. Nat. Cell Biol. *15*, 731–740. https://doi.org/10.1038/ncb2746.

Matson, J.P., Dumitru, R., Coryell, P., Baxley, R.M., Chen, W., Twaroski, K., Webber, B.R., Tolar, J., Bielinsky, A.-K., Purvis, J.E., and Cook, J.G. (2017). Rapid DNA replication origin licensing protects stem cell pluripotency. eLife *6*, e30473. https://doi.org/10.7554/eLife.30473.

Melixetian, M., Ballabeni, A., Masiero, L., Gasparini, P., Zamponi, R., Bartek, J., Lukas, J., and Helin, K. (2004). Loss of Geminin induces rereplication in the presence of functional p53. J. Cell Biol. *165*, 473–482. https://doi.org/10.1083/jcb.200403106.

Mougkogianni, M., Kalogeropoulou, A., Giakoumakis, N.N., Lygerou, Z., and Taraviras, S. (2021). In vivo imaging of DNA-bound minichromosome maintenance complex in embryonic mouse cortex. STAR Protoc. *2*, 100234. https://doi.org/10.1016/j.xpro.2020.100234.

Mukhtar, T., and Taylor, V. (2018). Untangling cortical complexity during development. J. Exp. Neurosci. *12*. 117906951875933. https://doi.org/10.1177/1179069518759332.

Muñoz, S., Búa, S., Rodríguez-Acebes, S., Megías, D., Ortega, S., de Martino, A., and Méndez, J. (2017). In vivo DNA Re-replication elicits lethal tissue dysplasias. Cell Rep. *19*, 928–938. https://doi.org/10.1016/j.celrep.2017.04.032.

Nieminuszczy, J., Schwab, R.A., and Niedzwiedz, W. (2016). The DNA fibre technique – tracking helicases at work. Methods *108*, 92–98. https://doi.org/10.1016/j.ymeth.2016.04.019.

Nishitani, H., Sugimoto, N., Roukos, V., Nakanishi, Y., Saijo, M., Obuse, C., Tsurimoto, T., Nakayama, K.I., Nakayama, K., Fujita, M., et al. (2006). Two E3 ubiquitin ligases, SCF-Skp2 and DDB1-Cul4, target human Cdt1 for proteolysis. EMBO J. *25*, 1126–1136. https://doi.org/10.1038/sj.emboj.7601002.

Nishitani, H., Taraviras, S., Lygerou, Z., and Nishimoto, T. (2001). The human licensing factor for DNA replication Cdt1 accumulates in G1 and is destabilized after initiation of S-phase. J. Biol. Chem. *276*, 44905–44911. https://doi.org/10.1074/jbc.M105406200.

Patmanidi, A.L., Champeris Tsaniras, S., Karamitros, D., Kyrousi, C., Lygerou, Z., and Taraviras, S. (2017). Concise review: geminin-A tale of two tails: DNA replication and transcriptional/epigenetic regulation in stem cells. Stem Cells *35*, 299–310. https://doi.org/10.1002/stem.2529.

Patterson, E.S., Waller, L.E., and Kroll, K.L. (2014). Geminin loss causes neural tube defects through disrupted progenitor specification and neuronal differentiation. Dev. Biol. *393*, 44–56. https://doi.org/10.1016/j.ydbio.2014.06.021.

Petropoulos, M., Champeris Tsaniras, S., Taraviras, S., and Lygerou, Z. (2019). Replication licensing aberrations, replication stress, and genomic instability. Trends Biochem. Sci. *44*, 752–764. https://doi.org/10.1016/j.tibs.2019.03.011.

Pilaz, L.-J., Patti, D., Marcy, G., Ollier, E., Pfister, S., Douglas, R.J., Betizeau, M., Gautier, E., Cortay, V., Doerflinger, N., et al. (2009). Forced G1-phase reduction alters mode of division, neuron number, and laminar phenotype in the cerebral cortex. Proc. Natl. Acad. Sci. *106*, 21924–21929. https://doi.org/10.1073/pnas.0909894106.

Poli, J., Tsaponina, O., Crabbé, L., Keszthelyi, A., Pantesco, V., Chabes, A., Lengronne, A., and Pasero, P. (2012). dNTP pools determine fork progression and origin usage under replication stress. EMBO J. *31*, 883–894. https://doi.org/10.1038/emboj.2011.470.

Pruitt, S.C., Bailey, K.J., and Freeland, A. (2007). Reduced Mcm2 expression results in severe stem/progenitor cell deficiency and cancer. Stem Cells *25*, 3121–3132. https://doi.org/10.1634/stemcells.2007-0483.

Rausch, C., Weber, P., Prorok, P., Hörl, D., Maiser, A., Lehmkuhl, A., Chagin, V.O., Casas-Delucchi, C.S., Leonhardt, H., and Cardoso, M.C. (2020). Developmental differences in genome replication program and origin activation. Nucleic Acids Res. *48*, 12751–12777. https://doi.org/10.1093/nar/gkaa1124.

Ravindran, E., Gutierrez de Velazco, C., Ghazanfar, A., Kraemer, N., Zaqout, S., Hanif, M., Mughal, S., Prigione, A., Li, N., Fang, X., et al. (2021). Homozygous mutation in MCM7 causes autosomal recessive primary microcephaly and intellectual disability. J. Med. Genet. *59*, 453–461. https://doi.org/10.1136/jmedgenet-2020-107518.

Rujano, M.A., Basto, R., and Marthiens, V. (2015). New insights into centrosome imaging in Drosophila and mouse neuroepithelial tissues. Methods Cell Biol. *129*, 211–227. https://doi.org/10.1016/bs.mcb.2015.04.005.

Saldivar, J.C., Cortez, D., and Cimprich, K.A. (2017). The essential kinase ATR: ensuring faithful duplication of a challenging genome. Nat. Rev. Mol. Cell Biol. *18*, 622–636. https://doi.org/10.1038/nrm.2017.67.

Salomoni, P., and Calegari, F. (2010). Cell cycle control of mammalian neural stem cells: putting a speed limit on G1. Trends Cell Biol. *20*, 233–243. https://doi.org/10.1016/j.tcb.2010.01.006.

Sankar, S., Patterson, E., Lewis, E.M., Waller, L.E., Tong, C., Dearborn, J., Wozniak, D., Rubin, J.B., and Kroll, K.L. (2017). Geminin deficiency enhances survival in a murine medulloblastoma model by inducing apoptosis of preneoplastic granule neuron precursors. Genes Cancer *8*, 725–744. https://doi.org/10.18632/genesandcancer.157.

Schultz, K.M., Banisadr, G., Lastra, R.O., McGuire, T., Kessler, J.A., Miller, R.J., and McGarry, T.J. (2011). Geminin-deficient neural stem cells exhibit normal cell division and normal neurogenesis. PLoS One *6*, e17736. https://doi.org/10.1371/journal.pone.0017736.

Schultz, L.B., Chehab, N.H., Malikzay, A., and Halazonetis, T.D. (2000). P53 binding protein 1 (53bp1) is an early participant in the cellular response to DNA double-strand breaks. J. Cell Biol. *151*, 1381–1390. https://doi.org/10.1083/jcb.151.7.1381.

Seo, S., Herr, A., Lim, J.-W., Richardson, G.A., Richardson, H., and Kroll, K.L. (2005). Geminin regulates neuronal differentiation by antagonizing Brg1 activity. Genes Dev. *19*, 1723–1734. https://doi.org/10.1101/gad.1319105.

Spella, M., Britz, O., Kotantaki, P., Lygerou, Z., Nishitani, H., Ramsay, R.G., Flordellis, C., Guillemot, F., Mantamadiotis, T., and Taraviras, S. (2007). Licensing regulators Geminin and Cdt1 identify progenitor cells of the mouse CNS in a specific phase of the cell cycle. Neuroscience *147*, 373–387. https://doi.org/10.1016/j.neuroscience.2007.03.050.

Spella, M., Kyrousi, C., Kritikou, E., Stathopoulou, A., Guillemot, F., Kioussis, D., Pachnis, V., Lygerou, Z., and Taraviras, S. (2011). Geminin regulates cortical progenitor proliferation and differentiation. Stem Cells *29*, 1269–1282. https://doi.org/10.1002/stem.678.

Stathopoulou, A., Roukos, V., Petropoulou, C., Kotsantis, P., Karantzelis, N., Nishitani, H., Lygerou, Z., and Taraviras, S. (2012). Cdt1 is differentially targeted for degradation by anticancer chemotherapeutic drugs. PLoS One *7*, e34621. https://doi.org/10.1371/journal.pone.0034621.

Stoeber, K., Tlsty, T.D., Happerfield, L., Thomas, G.A., Romanov, S., Bobrow, L., Williams, E.D., and Williams, G.H. (2001). DNA replication licensing and human cell proliferation. J. Cell Sci. *114*, 2027–2041.

Symeonidou, I.-E., Taraviras, S., and Lygerou, Z. (2012). Control over DNA replication in time and space. FEBS Lett. *586*, 2803–2812. https://doi.org/10.1016/j.febslet.2012.07.042.

Takahashi, T., Nowakowski, R.S., and Caviness, V.S. (1995). The cell cycle of the pseudostratified ventricular epithelium of the embryonic murine cerebral wall. J. Neurosci. Off. J. Soc. Neurosci. *15*, 6046–6057. https://doi.org/10.1523/jneurosci.15-09-06046.1995.

Técher, H., Koundrioukoff, S., Nicolas, A., and Debatisse, M. (2017). The impact of replication stress on replication dynamics and DNA damage in vertebrate cells. Nat. Rev. Genet. *18*, 535–550. https://doi.org/10.1038/nrg.2017.46.

Toledo, L.I., Altmeyer, M., Rask, M.-B., Lukas, C., Larsen, D.H., Povlsen, L.K., Bekker-Jensen, S., Mailand, N., Bartek, J., and Lukas, J. (2013). ATR prohibits replication catastrophe by preventing global exhaustion of RPA. Cell *155*, 1088–1103. https://doi.org/10.1016/j.cell.2013.10.043.

Uzquiano, A., Gladwyn-Ng, I., Nguyen, L., Reiner, O., Götz, M., Matsuzaki, F., and Francis, F. (2018). Cortical progenitor biology: key features mediating proliferation versus differentiation. J. Neurochem. *146*, 500–525. https://doi.org/10.1111/jnc.14338.

Vetro, A., Savasta, S., Russo Raucci, A., Cerqua, C., Sartori, G., Limongelli, I., Forlino, A., Maruelli, S., Perucca, P., Vergani, D., Mazzini, G., Mattevi, A., Stivala, L.A., Salviati, L., and Zuffardi, O. (2017). MCM5: a new actor in the link between DNA replication and Meier-Gorlin syndrome. Eur. J. Hum. Genet. EJHG *25*, 646–650. https://doi.org/10.1038/ejhg.2017.5.

Yellajoshyula, D., Patterson, E.S., Elitt, M.S., and Kroll, K.L. (2011). Geminin promotes neural fate acquisition of embryonic stem cells by maintaining chromatin in an accessible and hyperacetylated state. Proc. Natl. Acad. Sci. U S A *108*, 3294–3299. https://doi.org/10.1073/pnas.1012053108.